

Manuscript no.: PCP-2007-E-00249

Running title: Silencing of xanthine dehydrogenase in Arabidopsis

Corresponding author:

Atsushi Sakamoto

Department of Mathematical and Life Sciences

Graduate School of Science

Hiroshima University

1-3-1 Kagamiyama, Higashi-Hiroshima 739-8526

Japan

Tel: +81-82-424-7449

Fax: +81-82-424-0749

E-mail: ahkkao@hiroshima-u.ac.jp

Subject areas:

(4) Proteins, enzymes and metabolism

(1) Growth and development

Number of black and white figures: 3

Number of color figures: 2

Number of tables: 3

The RNAi-mediated Silencing of Xanthine Dehydrogenase Impairs Growth and Fertility and Accelerates Leaf Senescence in Transgenic Arabidopsis Plants

Ayami Nakagawa¹, Saori Sakamoto², Misa Takahashi^{1,2,3}, Hiromichi Morikawa^{1,2,3} and Atsushi Sakamoto^{1,2,3,*}

¹*Department of Mathematical and Life Sciences, Graduate School of Science, Hiroshima University, 1-3-1 Kagamiyama, Higashi-Hiroshima, 739-8526 Japan*

²*Department of Biological Science, Faculty of Science, Hiroshima University, 1-3-1 Kagamiyama, Higashi-Hiroshima, 739-8526 Japan*

³*Core Research for Evolutional Science and Technology (CREST) Project of Japan Science and Technology Agency (JST), Kawaguchi, 332-0012 Japan*

Abbreviations:

GS1, cytosolic glutamine synthetase; GS2, chloroplastic glutamine synthetase; RNAi, RNA interference; RNS, reactive nitrogen species; ROS, reactive oxygen species; RT-PCR, reverse transcription-PCR; *SAG*, senescence-associated gene; XDH, xanthine dehydrogenase; XO, xanthine oxidase; XOR, xanthine oxidoreductase.

Footnotes:

*Corresponding author: E-mail, ahkkao@hiroshima-u.ac.jp; Fax, +81-82-424-0749.

Abstract

Xanthine dehydrogenase (XDH) is a ubiquitous enzyme involved in purine metabolism which catalyzes the oxidation of hypoxanthine and xanthine to uric acid. Although the essential role of XDH is well documented in the nitrogen-fixing nodules of leguminous plants, the physiological importance of this enzyme remains uncertain in non-leguminous species such as Arabidopsis. To evaluate the impact of an XDH deficiency on whole-plant physiology and development in Arabidopsis, RNA interference (RNAi) was used to generate transgenic lines of this species in which *AtXDH1* and *AtXDH2*, the two paralogous genes for XDH in this plant, were silenced simultaneously. The nearly complete reduction in the total XDH protein levels caused by this gene silencing resulted in the dramatic overaccumulation of xanthine and a retarded growth phenotype in which fruit development and seed fertility were also affected. A less severe silencing of *XDH* did not cause these growth abnormalities. The impaired growth phenotype was mimicked by treating wild-type plants with the XDH inhibitor allopurinol, and was reversed in the RNAi transgenic lines by exogenous supplementation of uric acid. Inactivation of XDH is also associated with precocious senescence in mature leaves displaying accelerated chlorophyll breakdown and by the early induction of senescence-related genes and enzyme markers. In contrast, the XDH protein levels increase with the ageing of the wild-type leaves, supporting the physiological relevance of the function of this enzyme in leaf senescence. Our current results thus indicate that XDH functions in various aspects of plant growth and development.

Key words: Arabidopsis (*Arabidopsis thaliana*), plant growth and development, purine metabolism, senescence, xanthine dehydrogenase

Introduction

Xanthine oxidoreductase (XOR) is an archetypal member of the molybdo-flavoenzyme family, the members of which are widely distributed from bacteria to higher organisms (Bray 1975). Although XOR has broad specificities for both reducing and oxidizing substrates, its highest affinities are generally observed for hypoxanthine and xanthine, the final two metabolic intermediates in the purine degradation pathway that eventually leads to the formation of uric acid. Hence, XOR is generally accepted as the key enzyme in the terminal steps of purine nucleotide catabolism (Harrison 2002).

In eukaryotes, XOR is a homodimer comprising subunits of approximately 150-kDa each which act as separate catalytic units and possess three distinct types of redox-active cofactors: two non-identical iron-sulphur (Fe_2S_2 -type) clusters, a flavin adenine dinucleotide and a molybdopterin that are bound by their amino-terminal, central and carboxyl-terminal regions, respectively (Hille and Nishino 1995). The mammalian XORs, including those from bovine milk and rat liver, represent the most extensively studied types of this enzyme and are known to exist in two forms, xanthine dehydrogenase (XDH; EC 1.1.1.204) and xanthine oxidase (XO; EC 1.1.3.22), both of which are encoded by the same gene. The dehydrogenase is the predominant *in vivo* form of this enzyme from which the oxidase can be converted posttranslationally either through irreversible and limited proteolysis or by the reversible oxidation of sulfhydryl residues (Della Corte and Stirpe 1972, Amaya et al. 1990).

Although both forms of mammalian XOR catalyze the oxidative hydroxylation of their purine substrates, XDH preferentially uses NAD^+ as its physiological electron acceptor whereas XO transfers the reducing equivalents directly to molecular oxygen, generating superoxide radicals and hydrogen peroxide as byproducts (Hille and Nishino 1995). Superoxide production is also catalyzed by XDH due to its intrinsic NADH-oxidase activity

(Sanders et al. 1996). Recent studies have further suggested that, in addition to oxygen reduction, XO is capable of reducing organic nitrates as well as inorganic nitrate and nitrite, thence releasing nitric oxide under anaerobic conditions using either NADH or xanthine as a reducing agent (Millar et al. 1998, Zhang et al. 1998). Because these free radicals, collectively known as reactive oxygen and reactive nitrogen species (ROS/RNS), play a significant but paradoxical role in biological systems serving as deleterious toxins and as principal signaling molecules, XOR has received considerable attention in recent years as a potential source of ROS and RNS during cellular signaling, regulation and tissue damage (Harrison 2002).

In higher plants, XOR displays biochemical properties (molecular mass, substrate preference, cofactor requirements, etc.) that are similar to the corresponding mammalian enzyme, as revealed by studies of the XOR enzymes purified from wheat and from some legumes (Triplett et al. 1982, Montalbini 1998, Montalbini 2000, Sauer et al. 2002). A notable difference, however, is that the plant enzyme exists strictly as a dehydrogenase form and appears not to undergo conversion to the oxidase form (we thus exclusively refer to the plant enzyme as XDH hereafter). In contrast to the available biochemical identification, the molecular functions of the plant XDHs have only recently begun to be unraveled and the genome of the model plant *Arabidopsis thaliana* has been shown to possess two transcriptionally active copies of the XDH gene, *AtXDH1* and *AtXDH2*, which lie in a tandem orientation on chromosome IV (Hesberg et al. 2004).

In all living organisms, purines are consecutively synthesized and degraded as crucial components of nucleic acids, and nucleotides including adenine and guanine. In most plants, when adenine and guanine nucleotides are partially degraded to their cognate nucleosides and nucleobases, these compounds are either recovered through purine salvaging pathways or converge at their common intermediate, xanthine (Stasolla et al. 2003, Zrenner et al., 2006). Xanthine is the key starting compound of purine catabolism where XDH catalyzes the initial

oxidation to uric acid. Although uric acid is excreted with urine as the final catabolite in certain animals including humans and other primates, it is further oxidized in higher plants to urea and ureides such as allantoin and allantoate, and ultimately broken down into CO₂, ammonia and glyoxylate (Stasolla et al. 2003, Zrenner et al., 2006). These end products of plant purine catabolism are then presumably reutilized or reassimilated as carbon and nitrogen sources. Hence, one potentially important function of XDH might be to mediate the recycling of carbon and nitrogen to sustain plant growth and development, although no direct evidence has yet been presented for this.

Another physiologically important role of XDH has been suggested from the observations that its activity in plants is closely associated with a wide range of physiological processes that include pathogen defense (Montalbini 1992), hypersensitive cell death (Montalbini 1995), drought response (Yesbergenova et al. 2005) and natural senescence (Pastori and del Río 1997). These observations are particularly noteworthy in light of the recent demonstration that, like its mammalian counterparts, plant XDH can oxidize NADH and thus produce superoxide (Hesberg et al. 2004, Yesbergenova et al. 2005). This suggests that this enzyme is involved in biotic and abiotic stress responses by regulating intracellular ROS levels. However, the real contribution of XDH activity to these phenomena and its precise physiological role are still largely obscure.

To further investigate the physiological functions of the plant XDHs in our present study, we generated transgenic lines of the Arabidopsis plant in which RNA interference (RNAi) was used to significantly suppress the expression of *XDH* at the transcript, protein and activity levels. Our subsequent characterization of the phenotypes of these *XDH* RNAi lines indicates that the downregulation of this enzyme results in reduced growth, impaired fruit development and increased seed sterility under normal growth conditions. In addition, these silenced lines show a noticeable early-senescence phenotype. Such global impacts of XDH deficiency in

transgenic *Arabidopsis* strongly suggest the importance of this enzyme during plant growth and development.

Results

Generation of XDH RNAi transgenic plants

In the *Arabidopsis* genome, there are two highly homologous genes for XDH, *AtXDH1* and *AtXDH2*, arranged in tandem on chromosome IV and separated by about 700 bp (Hesberg et al. 2004). To perform reverse-genetic studies, we attempted to simultaneously disable both genes by RNAi, primarily focusing on *AtXDH1* which appears to play the more important role as it is expressed at higher levels and responds to various stress treatments (Hesberg et al. 2004). *Arabidopsis* plants were transformed by vacuum infiltration of *Agrobacterium tumefaciens*, with an intron-spliced hairpin RNA construct (pHG-XDH; Fig. 1A) that constitutively expresses an inverted repeat of 600 bp that spans exons 3 and 4 of *AtXDH1* and is under control of the cauliflower mosaic virus 35S promoter. Seeds from infiltrated plants were allowed to germinate and grow on selective medium, and the resultant kanamycin-resistant plants (T₁ generation) were examined by genomic PCR for the integration of the T-DNA. Sixteen individual plants were confirmed to harbor T-DNA insertions (data not shown). After self-crossing, the resulting T₂ transgenic lines were screened by reverse transcription-PCR (RT-PCR) for *AtXDH1*, and three independent lines (designated xdh2, xdh4 and xdh5) were identified that showed markedly reduced expression of *AtXDH1* relative to an internal control gene (Fig. 1B). We also examined the possibility of simultaneously silencing *AtXDH2* in the xdh2, xdh4 and xdh5 transgenic lines as the RNAi-targeted sequence within *AtXDH1* is highly homologous (92.8%) to the corresponding region of *AtXDH2*. Despite the weaker

expression in wild-type plants, the transcript abundance of *AtXDH2* apparently decreased in the three transgenic lines (Fig. 1B), indicating that the expression of *AtXDH2* was in fact downregulated by this transformation.

To examine whether the reduced transcript levels in the RNAi transgenic lines correlated with a reduction in the corresponding protein levels, immunoblotting analysis was performed using a polyclonal antibody directed against a synthetic oligopeptide corresponding to the last 15 C-terminal residues of AtXDH1. This antibody was authenticated by its immunoreactivity against a single polypeptide of the expected size (150 kDa) in total extracts from wild-type plants (Fig. 1C, upper panel). Because AtXDH1 and AtXDH2 share very similar primary sequences, including their C-terminal amino acids, this antibody would most likely recognize both proteins. Consistent with the results of our RT-PCR, immunodetection for T₃ transgenic lines revealed that these XDH proteins were significantly lowered in the *xdh2* line and undetectable in both *xdh4* and *xdh5* (Fig. 1C, upper panel). These results are therefore in good agreement with those obtained by in-gel staining for XDH activity, which detected a single intense and faint band for the wild-type and *xdh2* plants, respectively, but showed no observable signals for the *xdh4* and *xdh5* plants (Fig. 1C, lower panel). Hence, three independent RNAi transgenic lines were established in Arabidopsis that show stable heritability of the silencing effect upon the total XDH protein expression and activity levels, from mild (*xdh2* line) to severe (*xdh4* and *xdh5* lines). In our subsequent experiments, transgenic plants of the T₃ and T₄ generations were used.

Alteration in the vegetative and reproductive development of XDH RNAi transgenic plants

To examine the effects of RNAi-mediated XDH deficiency at whole-plant level in our transgenic Arabidopsis lines, the growth of these transgenic lines was compared with wild-type plants in terms of both vegetative and reproductive development under standard nutrient

medium and soil conditions. The germination frequency of the *XDH* RNAi transgenic lines was found to be similar to that of the wild-type plants. However, a growth phenotype in the severely silenced lines, *xdh4* and *xdh5*, became apparent in the 5-week-old plants which were smaller than wild-type and also showed a reduction in the size and number of rosette leaves (Figs. 2A, B). The impaired growth of these two lines was also statistically significant, and involved a reduction in the whole-plant biomass by 39% for *xdh4* ($P < 0.01$) and 31% for *xdh5* ($P < 0.05$), compared with wild-type plants on a dry matter basis (Table 1). In contrast, the growth phenotype of the mildly silenced *xdh2* line was less obvious (Fig. 2A, B) and the biomass production of these plants was indistinguishable from wild-type (Table 1).

To test whether the phenotype of the *xdh4* and *xdh5* lines could be replicated by an induced loss of XDH activity in wild type plants, wild-type seeds were allowed to germinate and grow in the presence of allopurinol [4-hydroxypyrazolo(3,4-*d*)pyrimidine], a structural analog of hypoxanthine with known potent inhibitory effects upon XDH (Hille and Massey 1981). As shown in Figure 2C, this exposure to allopurinol seriously retarded the growth of the wild-type seedlings in a concentration-dependent manner, consistent with our earlier finding that the XDH deficiency is responsible for the reduced growth phenotype of the severely silenced transgenic lines.

The effects of a severe XDH deficiency were also apparent in adult plants. Although flowering was induced at the same time in the *xdh4* and *xdh5* lines as in the wild-type plants under a long-day period, the final height of the transgenic plants was only about one half to two-thirds of wild-type, with considerably shorter and fewer stems (Fig. 2D). Fruit development was also found to be altered in these severely silenced lines as the lengths of the mature fruits were significantly shortened (Fig. 2E and Table 1) and the incidence of sterility increased by 4.1-fold for *xdh4* ($P < 0.05$) and 9.8-fold ($P < 0.001$) for *xdh5* (Fig. 2F and Table 1). In addition to this alteration in fruit morphology, fertile fruits from the *xdh4* and *xdh5* lines

contained significantly fewer seeds (Table 1).

The silencing of *XDH* in the *xdh4* and *xdh5* lines was further found to cause a decrease in seed weight even though the average length and width of the seeds did not differ from wild-type (Table 1). These defects in fruit and seed development were reproducible in wild-type plants when allopurinol was applied at the inflorescence stage, which rendered most of the fruit stunted and seedless (Fig. 2G). In the case of the mildly silenced *xdh2* line, there were no significant differences found when compared with the wild-type plants in terms of fruit development, sterility or seed characteristics (Table 1). Taken together, these results indicate that a severe *XDH* deficiency affects both vegetative and reproductive development in *Arabidopsis*.

Acceleration of natural leaf senescence in XDH RNAi transgenic plants

In addition to the pleiotropic effects that can be observed during the development of the *xdh4* and *xdh5* transgenic plants, there were also signs of an earlier onset of senescence compared with wild-type plants. The third rosette leaves of 3-week-old transgenic plants were visually indistinguishable from wild-type, but the same leaves of the *xdh4* and *xdh5* lines subsequently began to turn yellow whereas those of the wild-type and *xdh2* lines remained green (Fig. 3A). Concomitant with the visible yellowing, the chlorophyll content decreased by 10% for *xdh4* ($P < 0.05$) and 22% for *xdh5* ($P < 0.05$) when compared with age-matched wild-type plants (Table 2). It is unlikely, however, that the silencing affects chlorophyll synthesis because there were no statistically significant differences found between the chlorophyll content of the wild-type and these *XDH*-silenced lines prior to the onset of the early senescence symptoms (Table 2).

To further validate the early senescence phenotype of the *xdh2*, *xdh4* and *xdh5* plants, the relative expression levels of various senescence-related markers were determined in 3- and 6-

week-old plants derived from these lines and compared with wild-type plants of the same age. First, we investigated changes in the levels of glutamine synthetase (GS) isoforms in the mature leaves of each plant (third to sixth leaf). During natural leaf senescence, cytosolic GS (GS1) is induced whereas chloroplastic GS (GS2) is repressed with ageing (Kamachi et al. 1991, Kawakami and Watanabe 1988). Thus, the ratio of GS1 to GS2 can be used as predictive indicator of senescent behavior. Immunoblotting analysis using an anti-GS antibody (Sakamoto et al. 1990) was followed by densitometric scanning of the individual isoforms to calculate the GS1-to-GS2 ratio in each leaf sample. The results listed in Table 2 show that the initial ratios were almost identical between the wild-type and three silenced lines and that each of these plants showed enhanced GS1/GS2 ratios after 3 weeks of growth. However, the magnitude of this enhancement in the case of the silenced lines (ranging from 2.0- to 2.6-fold) was significantly greater than wild-type (1.5-fold).

Leaf senescence is also characterized by an increase in the expression of a multitude of genes that are often referred to as senescence-associated genes (*SAGs*; Lorman et al. 1994, Weaver et al. 1998). We therefore analyzed the transcript levels of two representative *SAGs*, *SAG12* and *SAG13*, by semi-quantitative RT-PCR analyses of the third leaves from 7-week-old plants (Fig. 3B). For both genes, the transcripts were found to accumulate at much higher levels in the three *XDH*-silenced lines compared with wild-type plants (10- to 20-fold for *SAG12* and 8- to 11-fold for *SAG13*). In addition, we found that there was a generally good correlation between the degree of transcript accumulation and the severity of silencing. Overall, these results provide further molecular evidence of the association of an early senescence phenotype in *XDH*-silenced *Arabidopsis* lines.

To gain additional insight into the physiological roles of *XDH* during natural leaf senescence in *Arabidopsis*, we investigated the distribution of *XDH* protein at three different stages of leaf development (senescent, mature and young) in both wild type and the *XDH*-

silenced plants. Immunoblotting analysis of wild-type plants revealed that XDH proteins are developmentally regulated and predominantly accumulate in mature and senescent leaves (Fig. 4A). We next monitored changes in the XDH protein levels during the ageing process of mature leaves and found that wild-type leaves showed increased levels of this protein in an age-dependent manner (Fig. 4B). In contrast, the *xdh2*, *xdh4* and *xdh5* silenced lines showed either a remarkably reduced or total loss of XDH in parallel experiments. We conclude therefore, that there is a positive correlation between the XDH protein levels and the progression of leaf ageing and senescence in wild-type leaves, whereas the absence of XDH is likely to be associated with the accelerated senescence phenotype in the silenced leaves. These data thus further suggest the involvement of XDH in the process of leaf senescence.

Xanthine accumulation in XDH RNAi transgenic plants

Because XDH is the only plant enzyme known to date that degrades xanthine, it was predicted that RNAi transgenic plants were blocked in xanthine metabolism and consequently accumulated this metabolic intermediate. To substantiate the prediction, we examined xanthine pools of Arabidopsis plants by performing HPLC analysis (Fig. 5). Apparently in close correlation with the reduction of XDH protein and activity, the three transgenic lines showed dramatically increased contents of xanthine compared with wild-type plants. There was more than a 30-fold overaccumulation in severely silenced *xdh4* and *xdh5* lines, and a significant but less dramatic accumulation (2.5-fold) was observed in mildly silenced *xdh2* lines. These results demonstrated that XDH activity was specifically disrupted in Arabidopsis plants by the coincident silencing of *AtXDH1* and *AtXDH2*. The observed biochemical phenotype of RNAi transgenic plants fits with the current knowledge on plant purine metabolism that xanthine is not the substrate for purine salvage reactions and only to be decomposed by XDH.

Restoration of the impaired growth phenotype of the XDH-silenced lines by treatment with uric acid

The germination and subsequent growth of wild-type plants were not significantly affected by the presence of nearly saturated concentrations (up to 0.4 mM) of xanthine under tissue culture conditions (data not shown). Thus, it is less likely that the growth phenotypes observed in our severely *XDH*-silenced lines were caused by the overaccumulation of xanthine. We therefore speculated that the growth defects might be attributable to a deficiency in uric acid as a result of the loss of XDH activity. To examine this possibility, seeds from both wild-type and silenced lines were germinated and grown in soil for 5 weeks during which the watering medium was supplemented with different concentrations of uric acid (Table 3). Under the control conditions (without uric acid), the biomass production of the *xdh4* and *xdh5* plants was significantly low, reaching only 55% and 48% of wild-type levels, respectively ($P < 0.05$ for both). In the presence of 100 μM of urate supplement, however, the impaired growth of these severely silenced lines was almost completely reversed with biomass yields of 96% and 89% for *xdh4* and *xdh5*, respectively, when compared with wild-type plants grown under urate-free conditions. Treatments with increased concentrations of urate of up to 200 μM resulted in similar reversing effects. Although the exogenous supplementation of uric acid seemed to inhibit the growth of WT plants, the differences in biomass were found to be insignificant between the control and metabolite-treated groups ($P \geq 0.05$). These results indicate that the defect in XDH activity leading to urate deficiency may be, at least in part, responsible for the appearance of the phenotypes observed in severely silenced lines during vegetative growth.

Discussion

XDH is one of the most widely studied enzymes in terms of its biochemistry and enzymology, and its role in purine degradation has been extensively characterized in both prokaryotes and eukaryotes. It has also been well documented that XDH is one of the key enzymes during the complex metabolism of purine compounds in the N₂-fixing nodules of ureide-producing legumes, where it plays an essential role in generating the major flow of fixed nitrogen for storage and transport to other tissues (Smith and Atkins 2002). In contrast, in plants that are not able to fix nitrogen, much less is known about the impact of XDH function, or the significance of its role in metabolic processes in the context of both whole-plant physiology and development. This is at least partly due to the fact that few molecular genetic studies of XDH have so far been undertaken in higher plants (Hesberg et al. 2004), and partly also because no mutants or transgenic plants with a convincing phenotype that specifically lack XDH have previously been described in detail (Leydecker et al. 1995, Sagi et al. 1999, Yesbergenova et al. 2005). In our current RNAi study, however, we demonstrate that XDH is required for the normal growth and development of Arabidopsis, thus providing the first direct evidence for a vital role of this enzyme during plant growth and development, and also in physiological processes such as leaf senescence. Efficient silencing observed in the RNAi transgenic plants suggests that XDH is probably not essential for Arabidopsis growth, although our results do not eliminate the possibility that the undetectable level of XDH activity might still have significant functions in the transgenic lines.

The simultaneous silencing of *AtXDH1* and *AtXDH2*, the two highly homologous paralogs present in the Arabidopsis genome, was obtained by expressing an intron-spliced *AtXDH1*-targeting hairpin RNA construct which led to the generation of three affected transgenic lines showing differing degrees of suppression of total XDH protein and activity. The total absence

of immunoblotting and in-gel activity signals (Fig. 1C) strongly indicates that XDH protein and activity levels are negligible or at least only marginal in severely silenced transgenic plants (*xdh4* and *xdh5* lines). Importantly, the induction of the pleiotropic phenotypes characterized by reduced biomass production, altered fruit development, and impaired fertility, was observed only in severely *XDH*-silenced lines which exhibited nearly complete loss of this enzyme. This observation points to a low threshold level and the requirement for a strong reduction in XDH activity to induce the observed phenotypes, although at the molecular level a silencing effect is evident even in the mildly silenced line (*xdh2*) as demonstrated by the early activation of senescence-related markers (Table 2, Fig. 3B).

There is some circumstantial evidence, most of which is derived from physiological studies employing XDH-inhibitors (Hammer et al. 1985, Atkins et al. 1988, Taylor and Cowan 2004, and herein), to suggest that the XDH enzyme plays a role in nitrogen recycling, thus contributing to plant growth and productivity (Stasolla et al. 2003, Zrenner et al., 2006). Taking this into account, our current observation that *XDH* RNAi transgenic plants show impaired vegetative and reproductive growth lead us to speculate that these phenotypes are directly or indirectly affected by the loss of the function of this enzyme which mediates the reassimilation of final purine catabolites such as ammonia. Both chlorophyll decomposition and the induction of senescence markers represent physiological responses to nitrogen limitation (Diaz et al. 2006, Masclaux-Daubresse et al. 2007), and the acceleration of these processes in our current RNAi transgenic plants (Table 2 and Fig. 3) is consistent with this possibility. This additionally implies that mature leaves of our *XDH* RNAi transgenic lines may have experienced a relative deficiency in an available nitrogen source during the course of ageing as compared with the wild-type leaves. Moreover, when we exogenously supplied uric acid, a metabolite of XDH reactions, this almost completely restored the wild-type phenotype in our RNAi transgenic plants during vegetative growth (Table 3), suggesting that

a metabolite deficiency causes the observed phenotype and that the efficient conversion of xanthine to metabolically active intermediates, such as ureides and urea, may play a role in ensuring the healthy growth of plants. Because of their low carbon-to-nitrogen ratios, these compounds have been considered to be a viable alternative nitrogen source in non-leguminous plants, particularly under nitrogen-deprived conditions. In fact, urea has been shown to be essential for the germination of *Arabidopsis* under nitrogen-limited conditions (Zonia et al. 1995), and recent reverse-genetic studies have also shown that the ureide compounds, allantoin and allantoate, can serve as the sole nitrogen source during the growth of *Arabidopsis* seedlings (Desimone et al. 2002, Yang and Han 2004, Todd and Polacco 2006).

Aside from its role in purine metabolism, much recent interest has been generated concerning the proposed role of XDH in the production of superoxide radicals as signaling messengers in various aspects of plant physiology and pathophysiology. This assumption is largely based on several observations that an increase in the mRNA levels and enzyme activity of XDH is closely associated with stress and other physiological conditions that involve the generation of ROS (Montalbini 1992, Montalbini 1995, Pastori and del Rio 1997, Hesberg et al. 2004, Yesbergenova et al. 2005). A recent demonstration of intrinsic NADH oxidase activity further supports the role of XDH as an ROS-generating enzyme (Hesberg et al. 2004, Yesbergenova et al. 2005). However, the pathophysiological role of XDH is still controversial (Ádám et al. 2000) and there is yet no solid evidence to conclude that elevated XDH levels indeed contribute to the ROS-mediated defense and acclimatization responses to biotic or abiotic stress in plants. In our present study, the physiological impact of the loss of *XDH* expression was evaluated under non-stress conditions, and the impaired growth of the *XDH* RNAi transgenic plants was restored by exogenous uric acid, which is also known as an efficient antioxidant scavenger. Thus, our results indicate that the purine catabolic activity of XDH, rather than its superoxide-generating capability, is the function of this enzyme that

plays a role in the growth and development of Arabidopsis plants. However, our results do not completely exclude the possibility that XDH serves also as an NADH oxidase to regulate ROS levels under certain physiological situations. Obviously, further studies will be needed to precisely define the contribution of these two discrete activities of XDH to the roles proposed for this classic enzyme with potentially multifaceted functions.

Materials and Methods

Plant materials and growth conditions

Wild-type *Arabidopsis* plants [*Arabidopsis thaliana* (L.) Heynh., accession C24] and three independent transgenic lines were used in the present study. The seeds in each case were soaked in 2.5% (v/v) sodium hypochlorite for 5 min and rinsed with 3 changes of sterile water for 10 min, during which the seeds imbibed. After 1 day of incubation in darkness at 4°C to break dormancy and to provide uniform germination, surface-sterilized seeds were sown on 0.3% (w/v) gellan gum plates in Petri dishes or Agripot containers (Kirin Brew Co., Tokyo, Japan) with Murashige and Skoog (MS) salts plus 1% (w/v) sucrose, pH 5.6. The plates were then placed in 16-h light (70 $\mu\text{mol photons m}^{-2} \text{s}^{-1}$) per day at a constant temperature of 22°C in growth chambers (MLR-350HT; Sanyo Electric Co., Tokyo, Japan). Aseptically cultured seedlings were then transferred to pots containing vermiculite and perlite (1:1 in volume) at 3 weeks following imbibition, and irrigated with half-strength MS salt solution every 5 days until harvesting for molecular and biochemical analysis, or growth to maturity and seed setting. The growth conditions were as described above. For the evaluation of biomass production, imbibed seeds were sown in pots and irrigated with half-strength MS salt solution supplemented with or without uric acid (100 or 200 μM ; Wako Pure Chemical Industries, Osaka, Japan) every 5 days. At 5 weeks following imbibition, the plants were harvested and the dry matter weights were determined in each case after lyophilization in a freeze dryer (VD-800F; Taitech, Koshigoe, Saitama, Japan). To examine the effects of allopurinol on the growth of wild-type plants, surface-sterilized seeds were sown on gellan gum-solidified MS medium supplemented with the defined concentrations of allopurinol (0.5, 1 or 2 mM; Sigma Chemicals Co., St. Louis, MO, USA), and allowed to grow for 4 weeks under sterile conditions. Alternatively, 18-day-old plants from aseptic culture were transferred to the soil

and irrigated with half-strength MS salt solution containing 50 μ M allopurinol every 5 days until inflorescence formation.

Construction of silencing vector

The target sequence for the induction of *XDH* RNAi in Arabidopsis was amplified by PCR and introduced into the hairpin RNA-expressing pHellsgate8 vector (Helliwell et al. 2002) using the Gateway™ system (Invitrogen, Carlsbad, CA, USA). Briefly, an expressed sequence tag clone (accession no. AV548322; Asamizu et al. 2000), comprising the complete open reading frame for AtXDH1 was obtained from the Kazusa DNA Research Institute.

Using this clone as a template, a 600-bp fragment of *AtXDH1* cDNA from nucleotides 262 to 861 (relative to the ATG start codon) was amplified using the primers, GW-AtXDH262FW (5'-GGGGACAAGTTTGTACAAAAAAGCAGGCTTACCAGTAGTTTTGCATCA-3') and GW-AtXDH262RE (5'-

GGGGACCACTTTGTACAAGAAAGCTGGGTTATTCTGTAGAAGGGATG-3'),

containing an *attB1* and *attB2* recombination site (underlined) at the 5' end, respectively. The PCR conditions consisted of an initial denaturation step for 2 min at 95°C, followed by 30 cycles of 15 s at 94°C, 30 s at 60°C, and 1 min at 72°C, with a final elongation step of 2 min at 72°C. The amplified PCR product was first cloned into the donor vector pDONR™221 (Invitrogen) to create an entry clone, and after sequence verification, the *AtXDH1* sequence was transferred to the binary T-DNA destination vector pHellsgate8 in reactions mediated by BP and LR Clonase™ (Invitrogen). The resulting recombinant construct, pHG-XDH, was then introduced into *Agrobacterium tumefaciens* C58C1Rif^R harboring the pMP90 helper plasmid (Koncz and Schell 1986) via a freeze-thaw method.

Generation of transgenic plants

Arabidopsis plants were transformed using the vacuum infiltration method as previously described (Bechtold et al. 1993). Briefly, *A. tumefaciens* carrying pHG-XDH were grown to stationary phase at 28°C in liquid YEB medium supplemented with 100 mg l⁻¹ rifampicin, 25 mg l⁻¹ gentamycin and 50 mg l⁻¹ kanamycin. These bacteria were then sedimented by centrifugation at 5,000 x g for 15 min at 28°C and resuspended in 5% (w/v) 2-(N-morpholino)-ethanesulfonic acid-KOH (pH 5.7) containing 5% (w/v) sucrose, half-strength MS salts, half-strength Gamborg's B5 vitamins, 44 nM benzyl aminopurine and 0.02% (v/v) Silwet L-77 (Dow Corning Toray Co. Ltd., Tokyo, Japan). Healthy flowering plants were immersed in the cell suspension, infiltrated for 10 min under a vacuum of 40 kPa, and then covered with plastic wrap for 3 days to prevent dehydration. The plants were then self-fertilized and seeds were collected in bulk from the dried fruits. To select transgenic plants (T₁ generation), the seeds from the infiltrated plants were germinated and tested for their antibiotic resistance on MS solid medium supplemented with 50 mg l⁻¹ kanamycin. T-DNA insertions in the kanamycin-resistant plants were verified by PCR amplification of genomic DNA.

Semi-quantitative RT-PCR analysis

Total RNA preparations were extracted from whole plants or leaves using the guanidium thiocyanate/acid phenol method. After heat denaturation at 65°C for 15 min, 0.5 µg aliquots of total RNA were reverse-transcribed at 42°C for 1 h with reverse transcriptases (ReverTra Ace; Toyobo, Osaka, Japan) and oligo-(dT) primers in a reaction volume of 20 µl. The resulting first-strand cDNAs were then diluted 10-fold, and 2 to 4 µl of these samples were subjected to PCR in a final volume of 20 µl. The following sets of primers were used to amplify cDNAs of interest: *AtXDHI* (At4g34890), *AtXDHFW* (5'-GGAGCGTTTGTACAAGGACT-3') and *AtXDH1RE* (5'-ACAATAGATTGATCGATCTG-3') amplifying a 456-bp fragment; *AtXDH2*

(At4g34900), AtXDHFW and AtXDH2RE (5'-GCGCATTTAGTCAACAAAGT-3') amplifying a 563-bp fragment; *SAG12* (At5g45890), SAG12FW (5'-GGCGGCTTGACAACTGAGTC-3') and SAG12RE (5'-TCATATAGTTGGGTAAGAAG-3') amplifying a 420-bp fragment; and *SAG13* (At2g29350), SAG13FW (5'-CACAACCTCCTTTAAGTAACG-3') and SAG13RE (5'-TTATGGCATAGTCTTGAAGG-3') amplifying a 200-bp fragment. As a control for the RT-PCR results, a 300-bp cDNA fragment of catalytic subunit A of the vacuolar ATP synthase (At1g78900; *AtVHA-A*) was co-amplified in each reaction with the primers AtVHA-AFW (5'-ATGCCGGCGTTTTACGGAGG-3') and AtVHA-ARE (5'-ATTTCCCAATATTCCTGGCC-3'). The parameters for the amplifications included preheating for 3 min at 94°C followed by following specific cycling conditions: for *AtXDHI*, 30 cycles of 94°C for 30 s, 54°C for 1 min and 72°C for 1 min; for *AtXDH2*, 35 cycles of 94°C for 30 s, 54°C for 1 min and 72°C for 1 min; for *SAG12*, 25 cycles of 94°C for 30 s, 52°C for 1 min and 72°C for 1 min; and for *SAG13*, 25 cycles of 94°C for 30 s, 54°C for 1 min and 72°C for 1 min. A final extension was performed in each case for 5 min at 72°C. The amounts of first-strand cDNA and the number of cycles used were chosen to ensure amplification within the linear range. Amplified PCR products of expected sizes were detected after electrophoresis in 8% (w/v) polyacrylamide gels stained with ethidium bromide. Quantification of the fluorescent signals was performed using a Gel Doc 2000 system and Quantity One software (Bio-Rad Laboratories, Hercules, CA, USA). Signal intensity was expressed as relative units, and the ratios between the amplified levels of each specific cDNA and *AtVHA-A* were calculated to normalize for initial variations in sample concentration.

Antibody production

A synthetic oligopeptide corresponding to the last 15 C-terminal residues of the AtXDH1 sequence (NH₂-Cys + SAPFVNSDFYPNLSV-COOH) was used as an immunogen

to generate specific antibodies and was conjugated with keyhole limpet hemocyanin via an added cysteine residue at the N-terminus. Rabbits were immunized subcutaneously with 0.5 mg of this immunogen at Shibayagi Co. Ltd. (Shibukawa, Gunma, Japan), and subsequently boosted in an identical manner five times at 2- to 3-week intervals.

SDS-PAGE and immunoblotting analysis

Whole plants or leaves were extracted with 2 volumes of 50 mM Tris-HCl (pH 8.0), 1 mM EDTA, 1 mM dithiothreitol and 1 mM phenylmethylsulfonyl fluoride, and then centrifuged at 14,000 $\times g$ for 20 min at 4°C. The protein concentration in the supernatants was determined with the Coomassie Plus™ Protein Assay Reagent (Pierce, Rockford, IL, USA) using bovine serum albumin (BSA) as the standard. Soluble proteins from whole plants (50 μg) or leaves (20 μg) were resolved by SDS-PAGE (7.5% separation gel, w/v) and then electrophoretically blotted onto polyvinylidene difluoride membranes (Immobilon™-P; Millipore, Bedford, MA, USA) for 1 h under constant current (2 mA cm^{-2} membrane) in 25 mM Tris and 192 mM glycine. The electroblotted membranes were blocked in phosphate-buffered saline (PBS; 10 mM potassium phosphate buffer, pH 7.4, 150 mM NaCl) containing 3% (w/v) BSA. For the detection of XDH, the specific primary antibody and a goat anti-rabbit IgG secondary antibody conjugated to horseradish peroxidase (Vector Laboratories, Burlingame, CA, USA) were used at 1:500 (v/v) and 1:2,000 (v/v) dilutions with PBS, respectively. For the detection of GS isoforms, a rabbit antibody raised against purified lettuce GS (Sakamoto et al. 1990) was diluted at 1:4,000 (v/v) and used as the primary antibody, after 3 μg of leaf proteins were subjected to SDS-PAGE (10% gel, w/v) that allowed electrophoretic separation of individual isoforms based on the differences in their molecular masses (GS1, 39 kDa; GS2, 43 kDa; Peterman and Goodman, 1991). The membranes were developed using the Western Lightning Chemiluminescence Reagent kit (Perkin-Elmer Life

Sciences, Boston, MA, USA) and the signals were quantified directly with a VersaDoc 5000 imaging system and Quantity One software (Bio-Rad Laboratories).

Native PAGE and in-gel activity staining

Four-week-old plants were ground into a fine powder in liquid nitrogen and soluble proteins were extracted as described above. An aliquot equivalent to 30 μ g of protein from each plant was then separated at 4°C on a 7.5% (w/v) native polyacrylamide gel under non-reducing conditions. Following electrophoresis, the gels were subjected to an in-gel procedure for NAD⁺-dependent dehydrogenase staining using nitroblue tetrazolium (NBT) to detect superoxide generation. The in-gel staining solution consisted of 50 mM Tris-HCl (pH 8.0), 0.1 mM NAD⁺, 0.1 mM NBT, 0.1 mM phenazine methosulfate and 1 mM hypoxanthine.

Determination of xanthine

Xanthine in whole plant samples was determined by HPLC analysis following perchloric acid extraction and partial purification by anion exchange column chromatography, with modification of the procedures described in Montalbini and Della Torre (1995) and Corpas et al. (1997). Six-week-old, aseptically grown plants (about 3 g) were extracted with an equal volume of 0.25 M perchloric acid and incubated for 15 min on ice. The homogenate was then centrifuged at 12,000 \times g for 15 min at 4°C to remove denatured proteins. The cleared supernatant was subsequently neutralized by adding approximately one-tenth volume of 2 M KOH and placed on ice to allow precipitation of potassium perchlorate. The neutralized sample was cleared by centrifugation, and the supernatant was lyophilized overnight. The dried residue was suspended in 0.5 M NaOH and centrifuged at 12,000 \times g for 5 min to remove residual potassium perchlorate. For further purification, the supernatant was loaded onto a Super Q anion exchange column (Tosoh Toyopearl SuperQ-650M; Tosoh Corp, Tokyo,

Japan) that was washed with methanol, and then the fraction containing xanthine was eluted with 1 M HCl. The fraction derived from the wild-type plants was subjected to lyophilization to concentrate the sample before the separation on an HPLC column.

Separation and quantification of xanthine were performed on a Shimadzu LC-10AD liquid chromatograph (Shimadzu Corp., Kyoto, Japan) equipped with an SCL-10A system controller, an SPD-10A UV-VIS spectrophotometric detector, an SIL-10A XL auto injector and a CTO-10ASVP column oven. The sample (20 μ l) containing xanthine was fractionated by HPLC on a reverse-phase Wakosil 5C18 column (250 mm long, 4.6 mm i.d., 25°C; Wako Pure Chemical Industries), eluted at a flow rate of 0.5 ml min⁻¹ with 50 mM sodium phosphate buffer (pH 2.5) containing 10 mM 1-hexanesulfonic acid and 1% (v/v) acetonitrile. The eluent was monitored at 260 nm to detect and quantify xanthine that has a retention time of 12.5 min under the condition described above. The authentic compound was obtained from Sigma Chemical Co.

Seed and fruit characteristics

Seed and fruit characteristics were analyzed for five plants per transgenic line, and a total of 10 fruits was collected from each plant under a stereomicroscope (Leica MZFLIII; Leica Microsystems, Wetzlar, Germany) by dissection from the primary inflorescent stem at positions between 6 and 16, counted from the lowest one. The collected fruits were then examined for the number of seeds contained in each. The average sizes of the seeds and fruits were determined by measurements of the length and width of 100 seeds (10 seeds per fruit) and the length of 10 fruits per plant using MetaMorph software (Molecular Devices Corporation, Downingtown, PA, USA) after digital images had been captured with scale under a stereomicroscope. Seed mass was determined by weighing mature dry seeds in batches of 100 using a microbalance (MT5; Mettler-Toledo, Leicester, UK). The incidence of

fruit sterility was calculated based on the ratio of completely empty fruits to the total number of fruits per plant.

Chlorophyll measurement

Chlorophyll was determined according to Lichtenthaler (1987) after extraction from fresh leaves in 80% (v/v) acetone. The absorbance of these extracts was then measured using a UV-VIS light spectrophotometer (BioSpec-1600; Shimadzu).

Statistical analysis

Data are presented as mean values \pm SD. Differences were evaluated for significance by means of Student's *t* test, with significance defined as $P < 0.05$ using a two-tailed unpaired *t* test.

Acknowledgments

We thank Dr. Takao Horikoshi of Hiroshima University (Higashi-Hiroshima, Japan) for the use of HPLC apparatus. We are also grateful to Kazusa DNA Research Institute (Kisarazu, Japan) for providing the AV548322 clone and to the CSIRO Plant Industry (Canberra, Australia) for providing the pHellsgate8 plasmid. This work was supported in part by a Grant-in-Aid for Scientific Research from the Japan Society for the Promotion of Science (grant no. 19570041 to A. S.).

References

- Ádám, A. L., Galal, A. A., Manniger, K. K. and Barna, B. (2000) Inhibition of the development of leaf rust (*Puccinia recondita*) by treatment of wheat with allopurinol and production of a hypersensitive-like reaction in a compatible host. *Plant Pathol.* 49: 317-323.
- Amaya, Y., Yamazaki, K., Sato, M., Noda, K., Nishino, T. and Nishino, T. (1990) Proteolytic conversion of xanthine dehydrogenase from the NAD-dependent type to the O₂-dependent type. Amino acid sequence of rat liver xanthine dehydrogenase and identification of the cleavage sites of the enzyme protein during irreversible conversion by trypsin. *J. Biol. Chem.* 265: 14170-14175.
- Asamizu, E., Nakamura, Y., Sato, S. and Tabata, S. (2000) A large scale analysis of cDNA in *Arabidopsis thaliana*: generation of 12,028 non-redundant expressed sequence tags from normalized and size-selected cDNA libraries. *DNA Res.* 7: 175–180.
- Atkins, C. A., Sanford, P. J., Paul, P. J., Storer, J. and Pate, J. S. (1988) Inhibition of nodule functioning in cowpea by a xanthine oxidoreductase inhibitor, allopurinol. *Plant Physiol.* 88: 1229-1234.
- Bechtold, N., Ellis, J. and Pelletier, G. (1993) *In planta Agrobacterium*-mediated gene transfer by infiltration of adult *Arabidopsis thaliana* plants. *C. R. Acad. Sci. Paris. Life Sci.* 316: 1194-1199.
- Bray, R. C. (1975) Molybdenum iron-sulfur flavin hydroxylases and related enzymes. In *The*

Enzymes, 3rd Edition. Edited by Boyer, P. D. Vol. XII, pp. 299-419. Academic Press, New York.

Corpas, F. J., de la Colina, C., Sánchez-Rasero, F. and del Río, L. A. (1997) A role for leaf peroxisomes in the catabolism of purines. *J. Plant Physiol.* 151: 246-250.

Della Corte, E. and Stirpe, F. (1972) The regulation of rat liver xanthine oxidase. Involvement of thiol groups in the conversion of the enzyme activity from dehydrogenase (type D) into oxidase (type O) and purification of the enzyme. *Biochem. J.* 126: 739-745.

Desimone, M., Catoni, E., Ludewig, U., Hilpert, M., Schneider, A., Kunze, R., Tegeder, M., Frommer, W. B. and Schumacher, K. (2002) A novel superfamily of transporters for allantoin and other oxo derivatives of nitrogen heterocyclic compounds in *Arabidopsis*. *Plant Cell* 14: 847-856.

Diaz, C., Saliba-Colombani, V., Loudet, O., Belluomo, P., Moreau, L., Daniel-Vedele, F., Morot-Gaudry, J.-F. and Masclaux-Daubresse, C. (2006) Leaf yellowing and anthocyanin accumulation are two genetically independent strategies in response to nitrogen limitation in *Arabidopsis thaliana*. *Plant Cell Physiol.* 47: 74-83.

Hammer, B., Liu, J. and Widholm, J. M. (1985) Effect of allopurinol on the utilization of purine degradation pathway intermediates by tobacco cell cultures. *Plant Cell Rep.* 4: 304-306.

Harrison, R. (2002) Structure and function of xanthine oxidoreductase: where are we now?

Free Rad. Biol. Med. 33: 774-797.

Helliwell, C. A., Wesley, S. V., Wielopolska, A. J. and Waterhouse, P. M. (2002) High-throughput vectors for efficient gene silencing in plants. *Funct. Plant Biol.* 29: 1217-1225.

Hesberg, C., Hansch, R., Mendel, R. R. and Bittner, F. (2004) Tandem orientation of duplicated xanthine dehydrogenase genes from *Arabidopsis thaliana*: differential gene expression and enzyme activities. *J. Biol. Chem.* 279: 13547-13554.

Hille, R. and Massey, V. (1981) Tight binding inhibitors of xanthine oxidase. *Pharm. Ther.* 14: 249-263.

Hille, R. and Nishino, T. (1995) Flavoprotein structure and mechanism. 4. Xanthine oxidase and xanthine dehydrogenase. *FASEB J.* 9: 995-1003.

Kamachi, K., Yamaya, T., Mae, T. and Ojima, K. (1991) A role for glutamine synthetase in the remobilization of leaf nitrogen during natural senescence in rice leaves. *Plant Physiol.* 96: 411-417.

Kawakami, N. and Watanabe, A. (1988) Senescence-specific increase in cytosolic glutamine synthetase and its mRNA in radish cotyledons. *Plant Physiol.* 88: 1430-1434.

Koncz, C. and Schell, J. (1986) The promoter T_L-DNA gene 5 controls the tissue-specific expression of chimeric genes carried by a novel type of *Agrobacterium* binary vector. *Mol Gen. Genet.* 204: 383-396.

- Leydecker, M.-T., Moureaux, T., Kraepiel, Y., Schnorr, K. and Caboche, M. (1995) Molybdenum cofactor mutants, specifically impaired in xanthine dehydrogenase activity and abscisic acid biosynthesis, simultaneously overexpress nitrate reductase. *Plant Physiol.* 107: 1427-1431.
- Lichtenthaler, H. K. (1987) Chlorophylls and carotenoids: pigments of photosynthetic biomembranes. *Methods Enzymol.* 148: 350-382.
- Lohman, K. N., Gan, S., John, M. C. and Amasino, R. M. (1994) Molecular analysis of natural leaf senescence in *Arabidopsis thaliana*. *Physiol. Plant.* 92: 322-328.
- Masclaux-Daubresse, C., Purdy, S., Lemaitre, T., Pourtau, N., Taconnat, L., Renou, J.-P. and Winkler, A. (2007) Genetic variation suggests interaction between cold acclimation and metabolic regulation of leaf senescence. *Plant Physiol.* 143: 434-446.
- Millar, T. M., Stevens, C. R., Benjamin, N., Eisenthal, R., Harrison, R. and Blake, D. R. (1998) Xanthine oxidoreductase catalyzes the reduction of nitrates and nitrite to nitric oxide under hypoxic conditions. *FEBS Lett.* 427: 225-228.
- Montalbini, P. (1992) Changes in xanthine oxidase activity in bean leaves induced by *Uromyces phaseoli* infection. *J. Phytopathol.* 134: 63-74.
- Montalbini, P. (1995) Effect of rust infection on purine catabolism enzyme levels in wheat leaves. *Physiol. Mol. Plant Pathol.* 46: 275-292.

Montalbini, P. and Della Torre, G. (1995) Allopurinol metabolites and xanthine accumulation in allopurinol-treated tobacco. *J. Plant Physiol.* 147: 321-327.

Montalbini, P. (1998) Purification and some properties of xanthine dehydrogenase from wheat leaves. *Plant Sci.* 134: 89-102.

Montalbini, P. (2000) Xanthine dehydrogenase from leaves of leguminous plants: purification, characterization and properties of the enzyme. *J. Plant Physiol.* 156: 3-16.

Pastori, G. M. and del Río, L. A. (1997) Natural senescence of pea leaves: an activated oxygen-mediated function for peroxisomes. *Plant Physiol.* 113: 411-418.

Peterman, T. K. and Goodman, H. M. (1991) The glutamine synthetase gene family of *Arabidopsis thaliana*: light-regulation and differential expression in leaves, roots and seeds. *Mol. Gen. Genet.* 230: 145-154.

Sagi, M., Fluhr, R. and Lips, S. H. (1999) Aldehyde oxidase and xanthine dehydrogenase in a *flacca* tomato mutant with deficient abscisic acid and wilted phenotype. *Plant Physiol.* 120: 571-577.

Sakamoto, A., Takeba, G. and Tanaka, K. (1990) Synthesis *de novo* of glutamine synthetase in the embryonic axis, closely related to the germination of lettuce seeds. *Plant Cell Physiol.* 31: 677-682.

Sanders, S. A., Harrison, R. and Eisenthal, R. (1996) Oxidation of NADH catalysed by human xanthine oxidase: generation of superoxide anion. *Biochem. Soc. Trans.* 24:13S.

Sauer, P., Frebortova, J., Sebel, M., Galuszka, P., Jacobsen, S., Pec, S. and Frebort, I. (2002) Xanthine dehydrogenase of pea seedlings: a member of the plant molybdenum oxidoreductase family. *Plant Physiol. Biochem.* 40: 393-400.

Smith, P. M. C. and Atkins, C. A. (2002) Purine biosynthesis. Big in cell division, even bigger in nitrogen assimilation. *Plant Physiol.* 128: 793-802.

Stasolla, C., Katahira, R., Thorpe, T. A. and Ashihara, H. (2003) Purine and pyrimidine nucleotide metabolism in higher plants. *J. Plant Physiol.* 160: 1271-1295.

Taylor, N. J. and Cowan, A. K. (2004) Xanthine dehydrogenase and aldehyde oxidase impact plant hormone homeostasis and affect fruit size in 'Hass' avocado. *J. Plant Res.* 117: 121-130.

Todd, C. D. and Polacco, J. C. (2006) *AtAAH* encodes a protein with allantoin amidohydrolase activity from *Arabidopsis thaliana*. *Planta* 223: 1108-1113.

Triplett, E. W., Blevins, D. G. and Randall, D. D. (1982) Purification and properties of soybean nodule xanthine dehydrogenase. *Arch. Biochem. Biophys.* 219: 39-46.

Weaver, L. M., Gan, S., Quirino, B. and Amasino, R. M. (1998) A comparison of the expression patterns of several senescence-associated genes in response to stress and hormone treatment. *Plant Mol. Biol.* 37: 455-469.

Yang, J. and Han, K.-H. (2004) Functional characterization of allantoinase genes from *Arabidopsis* and a nonureide-type legume black locust. *Plant Physiol.* 134: 1039-1049.

Yesbergenova, Z., Yang, G., Oron, E., Soffer, D., Fluhr, R. and Sagi, M. (2005) The plant Mo-hydroxylases aldehyde oxidase and xanthine dehydrogenase have distinct reactive oxygen species signatures and are induced by drought and abscisic acid. *Plant J.* 42: 862-876.

Zhang, Z., Naughton, D., Winyard, P. G., Benjamin, N., Blake, D. R. and Symons, M. C. R. (1998) Generation of nitric oxide by a nitrite reductase activity of xanthine oxidase: a potential pathway for nitric oxide formation in the absence of nitric oxide synthase activity. *Biochem. Biophys. Res. Commun.* 249: 767-772.

Zonia, L. E., Stebbins, N. E. and Polacco, J. C. (1995) Essential role of urease in germination of nitrogen-limited *Arabidopsis thaliana* seeds. *Plant Physiol.* 107: 1097-1103.

Zrenner, R., Stitt, M., Sonnewald, U. and Boldt, R. (2006) Pyrimidine and purine biosynthesis and degradation in plants. *Annu. Rev. Plant Biol.* 57: 805-836.

Table 1 Characterization of three *XDH* RNAi transgenic *Arabidopsis* lines

Plant line	Dry weight ^a (mg plant ⁻¹)	Fruit length ^b (mm)	Fruit sterility ^c (%)	Seed number per fruit ^d	Seed weight ^e (mg)	Seed length ^f (μ m)	Seed width ^f (μ m)
Wild-type	3.50 \pm 0.90 (<i>n</i> = 9)	16.6 \pm 0.5	1.5 \pm 0.9	47.8 \pm 2.0	2.22 \pm 0.24	514.0 \pm 24.4	299.0 \pm 16.9
xdh2	3.80 \pm 1.53 (<i>n</i> = 12)	14.8 \pm 2.1	2.1 \pm 1.9	44.2 \pm 4.7	2.30 \pm 0.32	503.0 \pm 8.3	279.0 \pm 10.2
xdh4	2.16 \pm 1.04* (<i>n</i> = 9)	12.8 \pm 1.1*	8.7 \pm 1.5*	36.8 \pm 1.7**	1.57 \pm 0.32**	453.5 \pm 23.3	247.0 \pm 15.8
xdh5	2.42 \pm 1.06* (<i>n</i> = 8)	12.3 \pm 1.4*	14.7 \pm 3.5**	31.8 \pm 3.7*	1.69 \pm 0.22**	505.8 \pm 26.8	294.8 \pm 29.5

^aWild-type and T₃ transgenic plants were grown in soil under long-day conditions at 22°C for 5 weeks, after which dry matter weights were determined.

^bA total of 10 mature fruits were collected from the main inflorescence per plant (*n* = 5), and their average lengths were determined using MetaMorph software (Molecular Devices) after digital images were captured under a stereomicroscope.

^cThe incidence of fruit sterility was calculated based on the number of seedless fruits versus the total number of fruits per plant (*n* = 5).

^dThe average number was determined for seeds contained in 10 mature fruits per plant (*n* = 5).

^eDry seed weight was measured for batches of 100 seeds per plant (*n* = 5).

^fAverage lengths and widths were determined for 100 seeds (10 per fruit) per plant using MetaMorph software (*n* = 5). The values shown are the means \pm SD with sample sizes given in parentheses, unless otherwise noted. Asterisks indicate statistical significance versus a wild-type control in each case (**P* < 0.05, ***P* < 0.001, Student's *t* test).

Table 2 Age-dependent changes in the chlorophyll content and GS1/GS2 ratio in the mature leaves of wild-type and *XDH* RNAi transgenic *Arabidopsis* lines

Plant line	3-week-old		6-week-old	
	Chlorophyll ^a (mg g ⁻¹ FW)	GS1/GS2 ^b	Chlorophyll ^a (mg g ⁻¹ FW)	GS1/GS2 ^b
Wild-type	3.25 ± 0.73	0.44 ± 0.13	1.53 ± 0.20	0.66 ± 0.16
<i>xdh2</i>	2.79 ± 0.60	0.46 ± 0.10	1.52 ± 0.24	0.90 ± 0.15*
<i>xdh4</i>	3.34 ± 0.51	0.42 ± 0.07	1.38 ± 0.26*	0.83 ± 0.08*
<i>xdh5</i>	3.04 ± 0.92	0.42 ± 0.08	1.19 ± 0.30*	1.08 ± 0.15*

^aChlorophyll was determined spectrophotometrically after extraction with 80% (v/v) acetone from the third rosette leaves ($n = 15$).

^bThe ratio of GS1 to GS2 was calculated based on quantification of immunoblotting signals for the individual isoforms extracted from the third to sixth rosette leaves ($n = 4$ and 3 for 3- and 6-week-old plants, respectively) by Quantity One software (Bio-Rad). Values are the means ± SD. Asterisks indicate statistical significance versus wild-type control in each case ($*P < 0.001$, Student's t test).

Table 3 Effects of uric acid treatments on the growth of wild-type and *XDH* RNAi transgenic *Arabidopsis* plants

Uric acid (μM)	Dry weight (mg plant^{-1})			
	Wild-type	<i>xdh2</i>	<i>xdh4</i>	<i>xdh5</i>
0	3.53 \pm 1.58 (<i>n</i> = 14)	3.54 \pm 1.32 (<i>n</i> = 15)	1.95 \pm 1.12* (<i>n</i> = 15)	1.70 \pm 1.01* (<i>n</i> = 15)
100	3.07 \pm 2.07 (<i>n</i> = 16)	4.37 \pm 2.13 (<i>n</i> = 18)	3.42 \pm 2.59 (<i>n</i> = 16)	3.17 \pm 1.51 (<i>n</i> = 15)
200	2.84 \pm 1.37 (<i>n</i> = 17)	3.86 \pm 1.73 (<i>n</i> = 15)	3.45 \pm 1.57 (<i>n</i> = 17)	2.49 \pm 1.60 (<i>n</i> = 18)

Wild-type and T₃ transgenic plants were grown in soil and irrigated with half-strength MS salt solution supplemented with or without the indicated concentrations of uric acid every 5 days under long-day conditions at 22°C. After 5 weeks of growth, plants were harvested and dry matter weights were recorded. Values are the means \pm SD with the sample sizes indicated in parentheses. Asterisks indicate statistical significance versus the uric acid-free wild-type control in each case (**P* < 0.05, Student's *t* test).

Figure Legends

Fig. 1 Generation of *XDH* RNAi transgenic *Arabidopsis* plants. (A) Schematic representation of the intron-exon organization of *AtXDH1* (top), structure of the corresponding mRNA (middle) and the T-DNA of the hairpin-RNA expression vector pHG-*XDH* (bottom). The target sequence (600 bp; between nucleotides 262 to 861 relative to the translation start site) is indicated by the box below the mRNA. The hairpin structure consisting of an antisense target sequence, pyruvate orthophosphate dikinase (PDK) intron, and the sense target sequence was inserted between the cauliflower mosaic virus 35S promoter (CaMV 35S *pro*) and the octopine synthase terminator (OCS *ter*) of the pHellsgate8 vector. Abbreviations: RB, right border; NOS *pro*, nopaline synthase promoter; *NPTII*, neomycin phosphotransferase II; NOS *ter*, nopaline synthase terminator; LB, left border. (B) Transcript levels of *AtXDH1* and *AtXDH2* in wild-type *Arabidopsis* plants (WT) and three independent transgenic *XDH* RNAi lines (*xhd2*, *xhd4* and *xhd5*) of the T₂ progeny. Total RNA from 4-week-old plants was analyzed by RT-PCR. *AtVHA-A* encoding the subunit A of vacuolar ATP synthase served as an internal control. (C) *XDH* protein and enzyme activity levels in wild-type and T₃ *XDH* RNAi transgenic plants. Total soluble extracts from 4-week-old plants were electrophoresed in 7.5% (w/v) polyacrylamide gels. For immunoblotting (upper panel), 50 µg of proteins were fractionated under reducing and denaturing conditions in the presence of SDS. For in-gel positive staining of *XDH* activity (lower panel), 30 µg of proteins were loaded under native conditions without SDS, and hypoxanthine and NBT were used as the substrate and chromogenic reagent, respectively.

Fig. 2 Phenotypes of the *XDH* RNAi transgenic *Arabidopsis* plants. Three lines of the T₃ generation (*xhd2*, *xhd4* and *xhd5*) are compared with wild-type plants (WT). (A) Five-week-

old soil-grown plants under long-day conditions. (B) Rosette leaves excised from 5-week-old plants. The first through tenth leaves from wild-type and *xdh2*, and through eighth from *xdh4* and *xdh5* are arranged from left to right in order of decreasing age. (C) Wild-type plants treated with various concentrations (0, 0.5, 1 and 2 mM) of the XDH inhibitor allopurinol after 4 weeks of aseptic growth under long-day conditions (D) Eight-week-old adult plants. (E) Fully expanded fruits. From left to right: wild-type, *xdh2*, *xdh4* and *xdh5*. (F) Primary inflorescences of an *xdh5* plant. Arrows indicate sterile fruits. (G) Primary inflorescences of a wild-type plant treated with 50 μ M allopurinol. Bars, 10 mm (A-C, F, G), 20 mm (D), 5 mm (E).

Fig. 3 The onset of leaf senescence in *XDH* RNAi transgenic *Arabidopsis* plants. (A) Visible leaf yellowing in the *xdh4* and *xdh5* lines. The third rosette leaves are shown from 3- and 6-week-old plants of wild-type and T₃ transgenic lines. Bar, 10 mm. (B) Transcript accumulation of the senescence-associated genes, *SAG12* and *SAG13*, in the *XDH* RNAi transgenic plants. The relative expression levels of *SAG12* and *SAG13* were examined by semi-quantitative RT-PCR analysis, using *AtVHA-A* as internal control, of the mature leaves of 7-week-old wild-type and T₃ transgenic plants. For each gene, the relative transcript levels detected in the wild-type plants were arbitrarily assigned a value of 1 after normalization to *AtVHA-A* in the same samples. The values shown are the means of three repeats \pm SD (indicated by error bars). Asterisks indicate statistical significance versus the wild-type control in each case (* $P < 0.05$, ** $P < 0.001$, Student's *t* test).

Fig. 4 Changes in the XDH protein levels during leaf development and ageing. (A) XDH protein levels at different leaf development stages. A total of 10 rosette leaves plus cotyledons from 4-week-old plants of wild-type and T₃ *XDH* RNAi transgenic lines were grouped into 3

age classes: senescent, cotyledons and first and second leaves; mature, third to sixth leaves; young, seventh to tenth leaves. Soluble extracts (20 µg of proteins) from each leaf class were subjected to immunoblotting after resolution by 7.5% SDS-PAGE. (B) Increases in XDH protein levels during the ageing process of mature leaves. Mature leaves were sampled from 3-, 6- and 7-week (wk)-old plants and analyzed as in (A).

Fig. 5 Xanthine accumulation in *XDH* RNAi transgenic Arabidopsis plants. Deproteinized extracts from 6-week-old plants of wild-type and T₄ transgenic lines were analyzed by reverse-phase HPLC as described in “Materials and Methods.” The values shown are the means of three repeats ± SD (indicated by error bars). Asterisks indicate statistical significance versus the wild-type plants (**P* < 0.05, ***P* < 0.01, Student’s *t* test). FW, fresh weight.

Figure 1 (Nakagawa et al.)

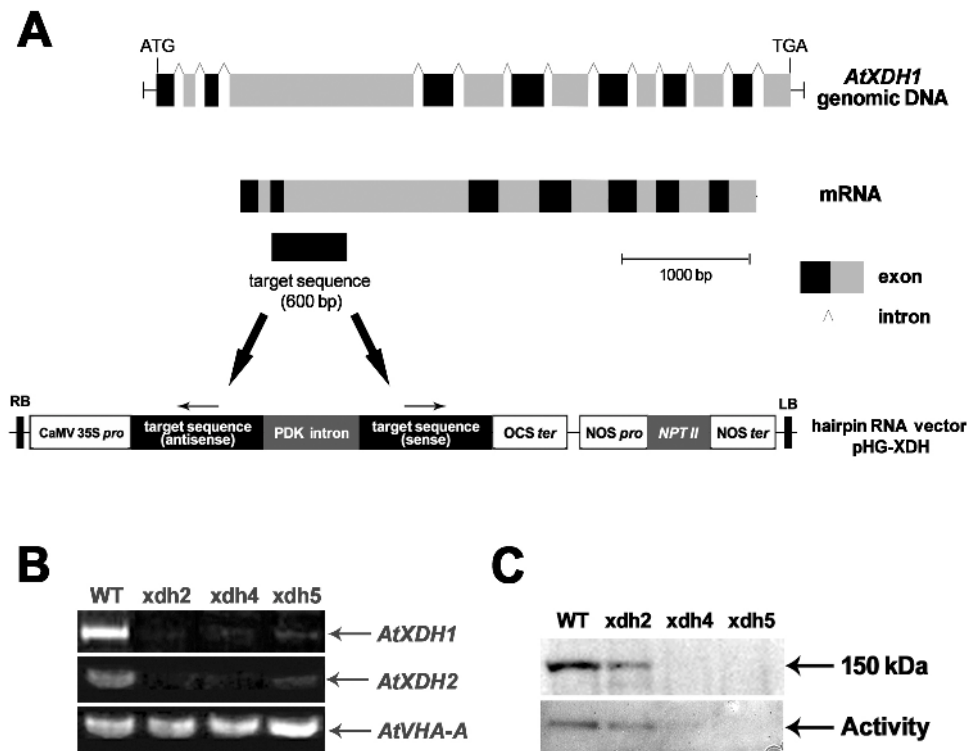


Figure 2 (Nakagawa et al.)

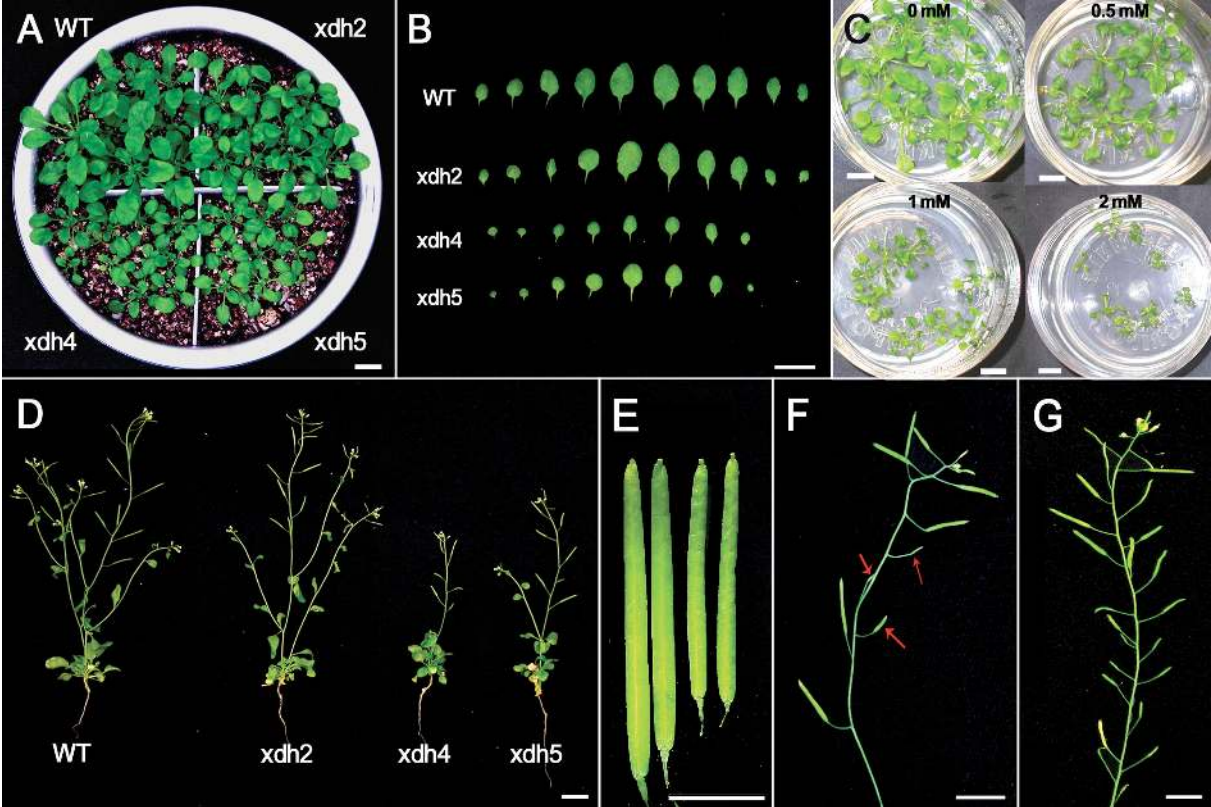


Figure 3 (Nakagawa et al.)

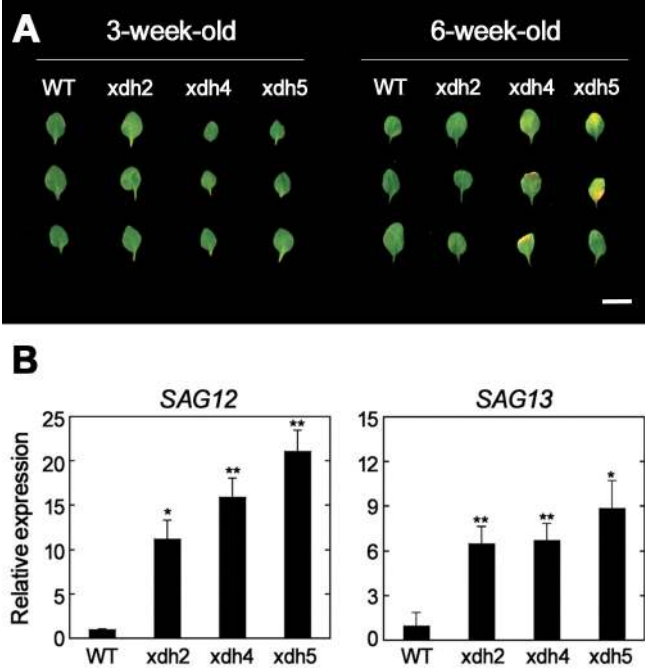


Figure 4 (Nakagawa et al.)

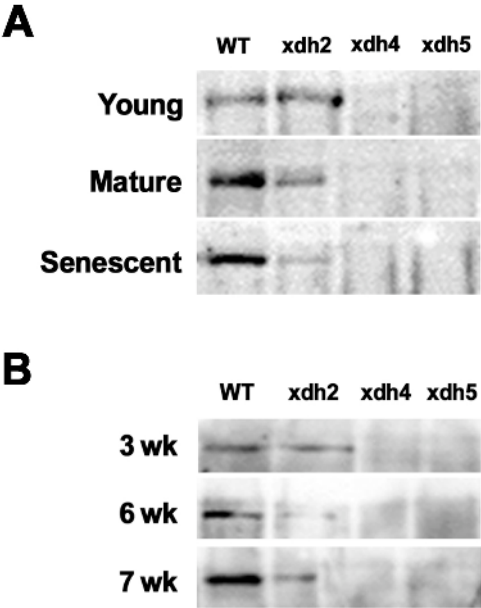


Figure 5 (Nakagawa et al.)

